Molecular Dynamics of Poly(ethylene glycol) and Poly(propylene glycol) Copolymer Networks by Broadband Dielectric Spectroscopy

Sumod Kalakkunnath,[†] Douglass S. Kalika,*[,†] Haiqing Lin,[‡,§] Roy D. Raharjo,[‡] and Benny D. Freeman[‡]

Department of Chemical and Materials Engineering and Center for Manufacturing, University of Kentucky, Lexington, Kentucky 40506-0046, and Center for Energy and Environmental Resources, Department of Chemical Engineering, University of Texas at Austin, Austin, Texas 78758

Received January 3, 2007; Revised Manuscript Received February 9, 2007

ABSTRACT: The dynamic relaxation properties of amorphous rubbery networks prepared by the UV photopolymerization of poly(ethylene glycol) diacrylate [PEGDA] and poly(propylene glycol) diacrylate [PPGDA] cross-linkers have been investigated using broadband dielectric spectroscopy. Effective cross-link density in the networks was controlled by copolymerization of the diacrylate cross-linkers with monofunctional acrylates of similar chemical composition. For all of the networks examined, three motional transitions were detected with increasing temperature, including an intermediate "fast" relaxation located between the typical sub-glass and glass−rubber processes and corresponding to a subset of constrained segmental motions that were more local and less cooperative in nature as compared to those associated with the glass transition. The properties of the intermediate relaxation were sensitive to the degree of constraint imposed by the cross-link junctions: the dielectric intensity of the fast process decreased with decreasing effective cross-link density, and the characteristic relaxation broadening associated with this transition was less pronounced in networks containing a lower degree of cross-linking. The intermediate process detected in the cross-linked networks was comparable to a distinct sub-glass dispersion measured in crystalline poly(ethylene oxide) [PEO] and which has been attributed to constrained motions originating in the vicinity of the crystal−amorphous interface.

Introduction

The dynamic relaxation properties of cross-linked polymer networks are highly sensitive to network composition and polymer chain architecture. Changes in backbone structure, cross-link density, or the introduction of pendant groups or branches can have a dramatic effect on the characteristics of the cooperative segmental motions associated with the glass transition as well as on the more localized processes observed below T_g. A broad literature has emerged that examines the underlying relationships between network structure, chain dynamics, and corresponding bulk properties in cross-linked polymer networks and which encompasses a number of fundamental dynamic characterization techniques. One of the most powerful and versatile methods for the measurement of molecular dynamics in polymer networks is broadband dielectric spectroscopy (BDS). The primary advantage of BDS is the exceptionally wide range of frequencies that can be accessed: commercial instruments provide for measurement from 10^{-5}−10^{7} Hz, and an overall range of up to 18 decades can be achieved by a combination of experimental configurations.[1,2] Dielectric spectroscopy has been used extensively for the characterization of polymer networks, as it can be applied to monitor the evolution of network formation in situ[3,4] as well as to elucidate polymer chain motions in the fully cured material as a function of temperature and time scale.

Recently, we have undertaken a systematic study of rubbery polymer networks based on the ultraviolet (UV) photopolymerization of poly(ethylene glycol) diacrylate [PEGDA] and poly(propylene glycol) diacrylate [PPGDA] cross-linkers.[5−15] These networks, which display high CO_2 permeability and favorable CO_2/light gas selectivity, hold considerable promise for use as CO_2-selective gas separation membranes. An important variable in the formulation of the networks is the effective cross-link density, which can be controlled by copolymerizing the diacrylate cross-linker with monofunctional acrylates of similar chemical composition. The stoichiometry of the copolymerization reaction leads to a systematic reduction in the number of cross-links as well as the insertion of fixed-length pendant or branch groups along the network backbone (see schematic of the resulting network in Figure 1.) The permeability and selectivity characteristics of the networks were investigated through a series of pure-gas and mixed-gas measurements that demonstrated the sensitivity of the transport properties to relatively subtle variations in network architecture.[7−10,13−15] Small differences in branch end group, for example, produced marked changes in the gas transport properties, suggesting that appropriate material design strategies could be employed to optimize gas separation performance.[10]

Three model copolymer network systems have been studied: PEGDA copolymerized with poly(ethylene glycol) methyl ether acrylate [PEGMEA], PEGDA copolymerized with poly(ethylene glycol) acrylate [PEGA], and PPGDA copolymerized with poly(propylene glycol) methyl ether acrylate [PPGMEA]. The corresponding chemical structures are shown in Table 1. In the case of the PEGDA/PEGMEA and PEGDA/PEGA copolymers, the molecular weights of the acrylates were selected so as to maintain an approximately constant ethylene oxide (EO) content in the copolymer networks (∼82 wt % EO), regardless of the ratio of monomers in the prepolymerization reaction mixture. For the PPGDA/PPGMEA networks, the molecular weight of the respective monomers was such that increasing the amount

* Corresponding author: Tel 859-257-5507; Fax 859-323-1929; e-mail kalika@engr.uky.edu.
[†] University of Kentucky.
[‡] University of Texas at Austin.
[§] Current address: Membrane Technology and Research, Inc., 1360 Willow Road, Suite 103, Menlo Park, CA 94025.

10.1021/ma070016a CCC: $37.00
Published on Web 03/17/2007

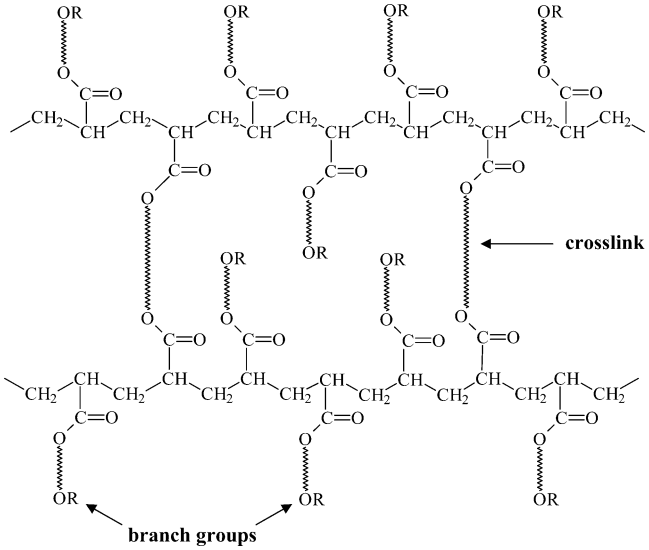

Figure 1. Schematic representation of ideal network based on the polymerization of diacrylate cross-linker and acrylate comonomer; −R corresponds to $-CH_3$ or −H.

Table 1. Chemical Structures of PEGDA and PPGDA Diacrylates; PEGMEA, PEGA and PPGMEA Acrylates (Monomeric Repeat Values (*n*) as Indicated)

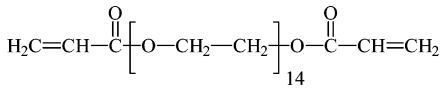

PEGDA

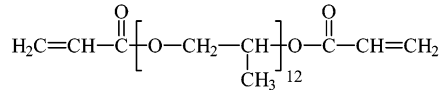

PPGDA

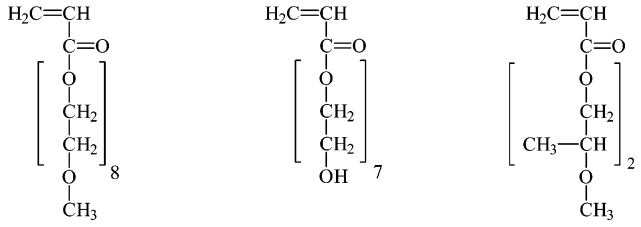

PEGMEA **PEGA** **PPGMEA**

of PPGMEA led to a decrease in overall propylene oxide (PO) content; PO content ranged from 60 to 85 wt % for the copolymer formulations examined.

A number of studies have examined the influence of cross-linking and related structural modifications on the segmental relaxation properties of polymer networks: dynamic mechanical analysis (DMA) and dielectric spectroscopy have been used to assess the effect of varying cross-link density on the glass transition temperature and corresponding time−temperature characteristics of the glass−rubber relaxation.[16−24] For the PEGDA and PPGDA networks investigated here, cross-link density is varied by the inclusion of monofunctional acrylate in the prepolymerization reaction mixture. The maximum cross-link density (or minimum distance between cross-links) is established by the molecular weight of the cross-linker. For PEGDA, the monomeric repeat length $n = 14$, while for PPGDA $n = 12$ (see Table 1). The acrylate comonomers, which contain repeating groups that match their respective cross-linker, act as chain extenders to reduce the effective cross-link density while simultaneously introducing fixed-length pendant groups along the $-(CH_2-CH_2)-$ network backbone. Previous dynamic mechanical studies on the PEGDA/PEGMEA,[11] PEGDA/PEGA,[11] and PPGDA/PPGMEA[15] networks provided detailed information on the glass−rubber relaxation characteristics of the copolymers and their relation to effective cross-link density. However, DMA offered relatively little insight as to how the sub-glass transitions operative in these materials were affected by variations in network structure, since these sub-glass processes involve localized motions that have only a very weak influence on bulk mechanical properties.[11,12] By contrast, dielectric spectroscopy has proven to be highly effective in probing the details of the sub-glass relaxations in these polymers. In a companion paper, we have recently reported the dielectric relaxation characteristics of 100% cross-linked networks based on PEGDA and PPGDA (i.e., XLPEGDA and XLPPGDA, where "XL" indicates cross-linked) as well as for crystalline PEO.[25] Each of these materials display three distinct dielectric relaxations with increasing temperature: two sub-glass transitions (labeled as the β_1 and β_2 processes) and the glass−rubber transition (labeled as the α process). In their study on the dielectric relaxation properties of PEO, Jin et al. assigned the intermediate β_2 process to an apparent subset of amorphous-phase segmental motions originating in the vicinity of the crystal−amorphous interface.[26] Owing to the constraint imposed by the crystal lamellar surfaces and corresponding conformational limitations experienced by the responding chain segments, a faster, more localized process emerges at temperatures below the glass transition. A comparable process is observed in both the XLPEGDA and XLPPGDA networks, presumably originating in the constrained regions near the cross-link junctions.[25] An analogy has been drawn between the "fast" relaxation observed in PEO and the networks, and a similar process identified in PEO-based nanocomposites where noncrystalline PEO is confined on the nanoscale within intercalated regions.[27,28]

In this paper, we examine the dielectric relaxation characteristics of three series of UV-polymerized rubbery copolymer networks as a function of varying cross-link density: PEGDA/PEGMEA, PEGDA/PEGA, and PPGDA/PPGMEA. For the two PEGDA series, the molecular weights of the acrylate comonomers (i.e., PEGMEA, PEGA) were intentionally chosen so as to maintain an approximately constant EO content in the networks while simultaneously inserting relatively long, flexible PEG branches into the network architecture; this approach facilitates the interpretation of changes in network dielectric response independent of variations in overall composition. The PPGDA/PPGMEA series, by contrast, has relatively short ($n = 2$) pendant groups positioned along the backbone in a network that contains a significantly higher fractional free volume as compared to the PEGDA copolymers. The measurement of dielectric response for these families of materials provides useful insights as to the effect of cross-linking and associated constraints on their sub-glass and glass−rubber relaxation characteristics, and how variations in cross-linking influence the static and dynamic properties of the networks and their ultimate gas separation performance.

Experimental Section

Materials. Poly(ethylene glycol) diacrylate [PEGDA; MW = 700 g/mol)] and poly(propylene glycol) diacrylate [PPGDA; MW = 900 g/mol] cross-linkers were obtained from Aldrich Chemical Co. (Milwaukee, WI) along with poly(ethylene glycol) methyl ether acrylate [PEGMEA; MW = 460 g/mol], poly(ethylene glycol) acrylate [PEGA; MW = 380 g/mol], and poly(propylene glycol)

methyl ether acrylate [PPGMEA; MW = 202 g/mol]. 1-Hydroxylcyclohexyl phenyl ketone [HCPK] initiator was also purchased from Aldrich. All reagents were used as received.

The molecular weights of the diacrylate cross-linkers and monofunctional acrylates were characterized using proton nuclear magnetic resonance (^{1}H NMR) and fast atom bombardment mass spectrometry (FAB-MS) in order to verify the values provided by the supplier; complete details of these characterizations have been reported previously.[9,11,15] The number-averaged molecular weight for each reactant is indicated by the value of the monomeric repeat, *n*, as shown in Table 1. For all reactants, FAB-MS measurements indicated a narrow distribution of molecular weight (polydispersity index <1.10).[9,15]

Copolymer Film Preparation. Cross-linked copolymer films were prepared by UV photopolymerization. A liquid prepolymer mixture comprised of diacrylate cross-linker (i.e., PEGDA or PPGDA) and acrylate comonomer (PEGMEA, PEGA, or PPGMEA) was blended in the desired ratio with 0.1 wt % HCPK initiator. The resulting mixture was sandwiched between two quartz plates which were separated by spacers to control film thickness. The mixture was polymerized by exposure to 312 nm UV light in a UV cross-linker (model FB-UVXL-1000, Fisher Scientific) for 90 s at 3 mW/cm^2. The solid films obtained by this procedure were three-dimensional networks and contained a negligible amount of low molecular weight polymer (i.e., sol) that was not bound to the network. In order to remove any residual sol or unreacted cross-linker, the films were washed with toluene in a Soxhlet extractor (Chemglass) for 1 day. Film thickness for the cross-linked networks was $\sim$350 μm; the precise thickness for each film was measured using a digital micrometer readable to $\pm$1 μm.

The extent of the polymerization reaction in the cross-linked polymer films was determined using FTIR-ATR spectroscopy (Nexus 470 spectrometer from Thermo Nicolet, Madison, WI); full details for these copolymer series were reported previously.[9,15] For all films studied here, essentially 100% conversion of the acrylate species was achieved, with no variation evident as a function of film depth.

Dielectric Relaxation Spectroscopy. Dielectric spectroscopy measurements were performed using the Novocontrol Concept 40 broadband dielectric spectrometer (Hundsangen, Germany). In order to ensure optimum electrical contact during measurement, concentric silver electrodes (33 mm diameter) were vacuum-evaporated on each polymer sample using a VEECO thermal evaporation system. Samples were then mounted between gold platens and positioned in the Novocontrol Quatro Cryosystem. All samples were rigorously dried under vacuum prior to measurement, and sample mounting procedures were designed to minimize exposure to ambient moisture. Dielectric constant (ϵ') and loss (ϵ'') were recorded in the frequency domain (0.1 Hz$-$1.0 MHz) at discrete temperatures from $-$150 to 100 °C.

Results and Discussion

Properties of PEGDA/PEGMEA, PEGDA/PEGA, and PPGDA/PPGMEA Copolymers. UV photopolymerization of the PEGDA/PEGMEA, PEGDA/PEGA, and PPGDA/PPGMEA prepolymerization mixtures led to the formation of amorphous rubbery polymer networks with 100% conversion of the acrylate and diacrylate end groups as verified by FTIR-ATR. The calorimetric glass transition temperatures (T_g) and fractional free volume (FFV) values associated with each network series have been reported in previous papers[10,11,15] and are summarized in Table 2. The copolymerization of PEGDA with either PEGMEA ($n = 8$) or PEGA ($n = 7$) leads to a progressive reduction in T_g, with the effect appearing more strongly in the PEGDA/PEGMEA copolymers. There is a distinct contrast in the fractional free volume trends associated with the two series: FFV in the PEGDA/PEGMEA copolymers increases with increasing comonomer (i.e., branch) content, while FFV in the PEGDA/PEGA series decreases with comonomer content, possibly due to the formation of hydrogen bonds involving the $-$OH terminal group present on the PEGA monomer. This difference in free volume characteristics appears to be a decisive factor in the resulting gas permeability properties of the networks.[10] For the PPGDA/PPGMEA copolymers, T_g is independent of copolymer composition, with the short PPGMEA branches having little apparent influence on the glass transition properties of the high free volume PPGDA networks. However, FFV in the PPGDA networks increases strongly with comonomer content, and this increase is reflected in systematically higher permeability values.[15]

Table 2. Characteristics of Cross-Linked PEGDA[10,11] and PPGDA[15] Copolymer Networks: Calorimetric Glass Transition Temperature and Estimated Fractional Free Volume

	T_g (°C)	FFV[a]
XLPEGDA	−40	0.118
PEGDA/PEGMEA[b]		
80/20	−44	0.122
50/50	−52	0.127
30/70	−57	0.128
PEGDA/PEGA[b]		
80/20	−40	0.112
50/50	−42	0.112
30/70	−44	0.110
XLPPGDA	−43	0.160
PPGDA/PPGMEA[b]		
50/50	−44	0.179
30/70	−43	0.190
9/91	−44	0.194

[a] FFV values based on bulk density measurements at 25 °C; see ref 10. [b] Copolymer compositions are reported on a wt % basis.

Dielectric Results for PEGDA/PEGMEA and PEGDA/PEGA Copolymers. Dielectric measurements for the PEGDA/PEGMEA and PEGDA/PEGA copolymer networks reveal three motional transitions with increasing temperature, and these have been labeled as the β_1, β_2, and α relaxations. Representative contour plots for the PEGDA/PEGMEA copolymer series are shown in Figure 2 (50/50 wt % PEGDA/PEGMEA network composition), with dielectric constant (ϵ') and loss (ϵ'') plotted vs temperature vs frequency. The observed sub-glass processes merge into a single relaxation with increasing frequency, and the combined (β) process eventually merges with the (glass$-$rubber) α process at the highest frequencies measured. The increase in dielectric loss at low frequency and high temperature (i.e., on the far left side of Figure 2b) reflects the onset of conduction associated with the transport of mobile charge carriers in the rubbery amorphous matrix.[29] Similarly, the influence of electrode polarization is apparent in the values of the dielectric constant at higher measurement temperatures.

Analysis of Sub-Glass Relaxations for PEGDA Copolymers. The intensity and breadth of the sub-glass relaxations in the PEGDA copolymers are sensitive to the degree of local constraint experienced by the responding dipolar moieties. In our previous dielectric studies on 100% XLPEGDA and XLPPGDA, we reported that the characteristics of the (higher temperature) β_2 sub-glass relaxation in the cross-linked networks were similar in many respects to an intermediate "fast" relaxation process detected in crystalline PEO.[25] In their analysis of dielectric dispersions observed in PEO samples with various thermal histories, Jin et al. identified a relaxation process with local Arrhenius character positioned between the sub-glass and glass$-$rubber relaxations that was assigned to segmental motions occurring in the vicinity of the crystal$-$amorphous interface.[26] It was proposed that this relaxation emerges as a result of

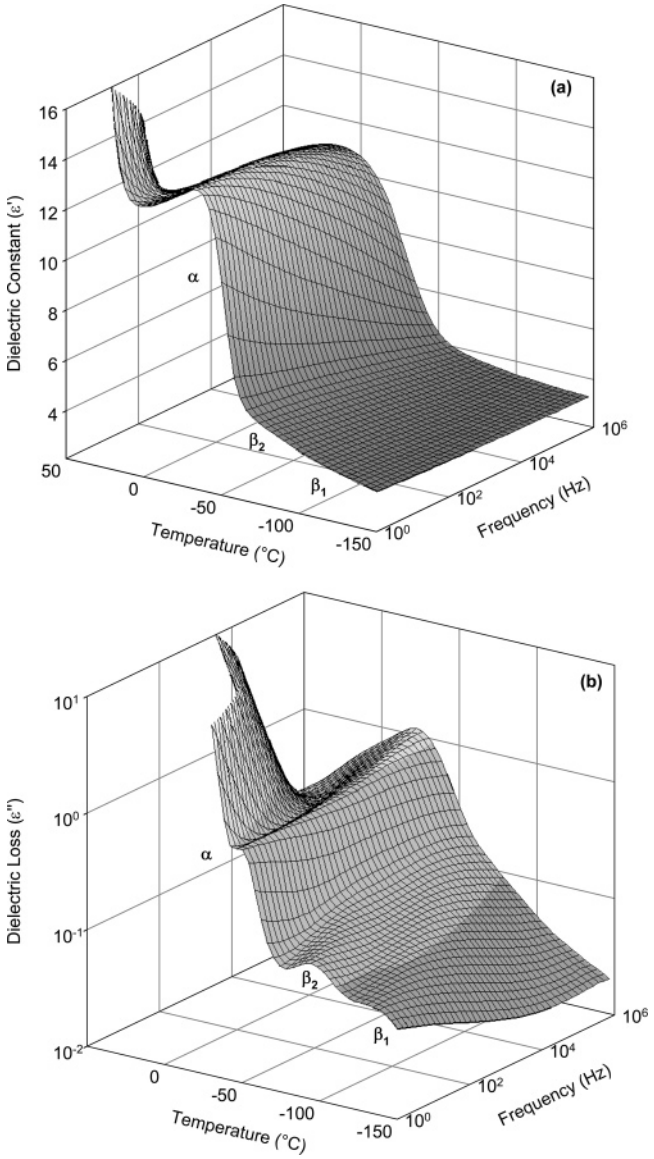

Figure 2. Contour plot of dielectric response for 50/50 (wt %) PEGDA/PEGMEA network: **(a)** dielectric constant (ϵ') vs temperature (°C) vs frequency (Hz); **(b)** dielectric loss (ϵ'') vs temperature (°C) vs frequency (Hz).

confinement effects which influence local chain conformation, and corresponds to a subset of segmental motions that in the absence of constraint would be shifted to longer relaxation times (i.e., higher temperatures) and would contribute to the glass−rubber relaxation of the bulk amorphous phase. Our measurements on the XLPEGDA and XLPPGDA networks suggest that this is a general phenomenon, with a separate "fast" segmental process evident in PEO and poly(propylene oxide) [PPO] materials subject to local constraints, including crystalline samples, chemically cross-linked networks, and nanocomposites.

A distinguishing feature of the β_2 dispersion in PEO is its breadth: Cole−Cole analysis indicated a broadening of the β_2 relaxation with increasing temperature that is opposite the trend usually observed in polymers, where the sub-glass and glass−rubber relaxations narrow with increasing thermal energy.[30] It has been proposed that this distinctive behavior for the β_2 relaxation in PEO reflects the inherent environmental asymmetry that exists between the amorphous and crystalline phases.[26] As the temperature of the polymer increases, this asymmetry becomes more pronounced, leading to a broader relaxation. A similar broadening of the β_2 process with increasing temperature

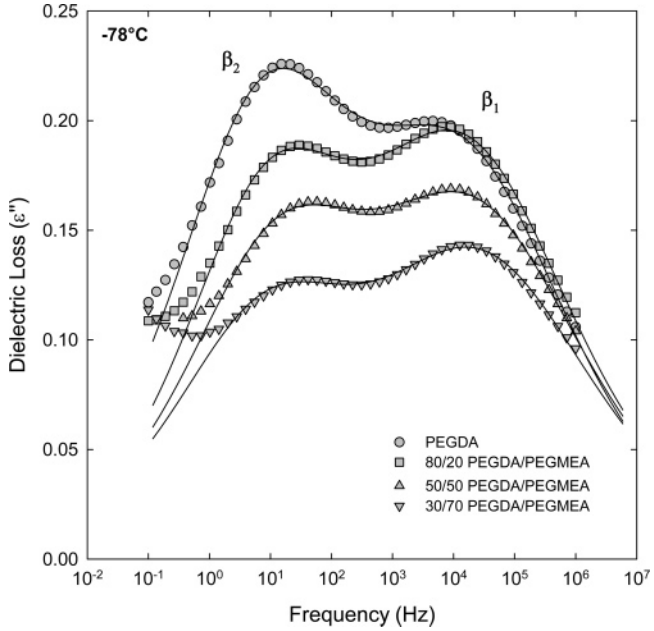

Figure 3. Dielectric loss (ϵ'') vs frequency for PEGDA/PEGMEA copolymer networks at −78 °C. Solid curves are dual HN fits.

was observed in the 100% cross-linked XLPEGDA and XLPPGDA networks.

Dielectric loss (ϵ'') for the PEGDA/PEGMEA copolymer series is plotted vs frequency in Figure 3; the selected temperature (−78 °C) corresponds to the midrange of the sub-glass transitions. The data reveal a strong sensitivity of the β_2 relaxation intensity to copolymer composition. Increasing the amount of PEGMEA comonomer in the prepolymerization reaction mixture leads to a marked decrease in β_2 relaxation intensity for the resulting copolymer films. This outcome suggests that as the PEGMEA branch content increases, and the corresponding cross-link density decreases, the overall constraint imposed by the cross-link junctions is diminished. As the constraint imposed by the cross-link junctions is loosened, fewer segments assume the restricted conformations associated with the β_2 process. With less local confinement, some portion of the segments originally associated with the β_2 process in the fully cross-linked (100% PEGDA) network adopt a conformation closer to that of the amorphous bulk, and consequently, a smaller portion of the responding segments contribute to the "fast" β_2 process, leading to a reduction in the measured β_2 intensity.

In order to objectively establish the characteristics of the individual sub-glass relaxations, the β_1 and β_2 loss data were fit in the frequency domain according to a dual Havriliak−Negami (HN) model:[31,32]

$$\epsilon^* = \epsilon' - i\epsilon'' = \epsilon_{U_1} + \sum_{i=1}^{2} \frac{\epsilon_{R_i} - \epsilon_{U_i}}{[1 + (i\omega\tau_{\mathrm{HN}_i})^{a_i}]^{b_i}} \qquad (1)$$

where ϵ_R and ϵ_U represent the relaxed ($\omega \rightarrow 0$) and unrelaxed ($\omega \rightarrow \infty$) values of the dielectric constant for each individual relaxation, $\omega = 2\pi f$ is the frequency, τ_{HN} is the relaxation time for each process, and a and b represent the broadening and skewing parameters, respectively. All curve fits reported here were obtained using the WinFIT software package provided with the Novocontrol dielectric spectrometer. For the sub-glass relaxations, it was observed that satisfactory fits to the dielectric dispersions could be obtained with the skewing parameter (b)

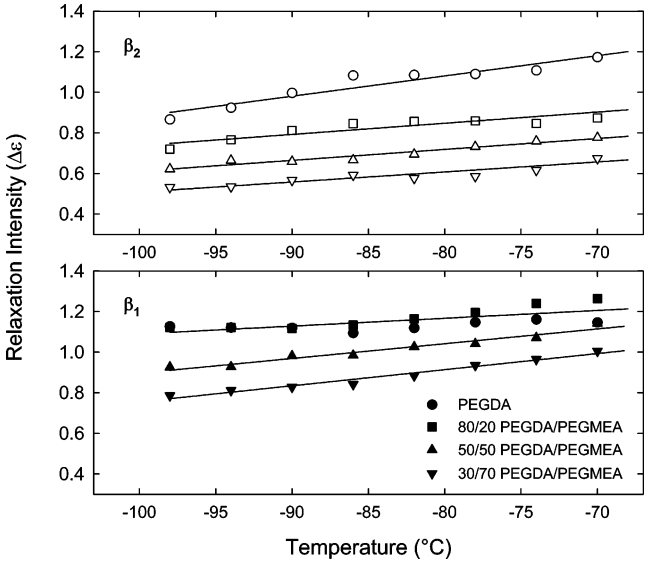

Figure 4. Dielectric relaxation intensity ($\Delta\epsilon$; determined from HN fits) vs temperature for PEGDA/PEGMEA copolymer networks: β_1 [filled symbols] and β_2 [unfilled symbols] sub-glass transitions.

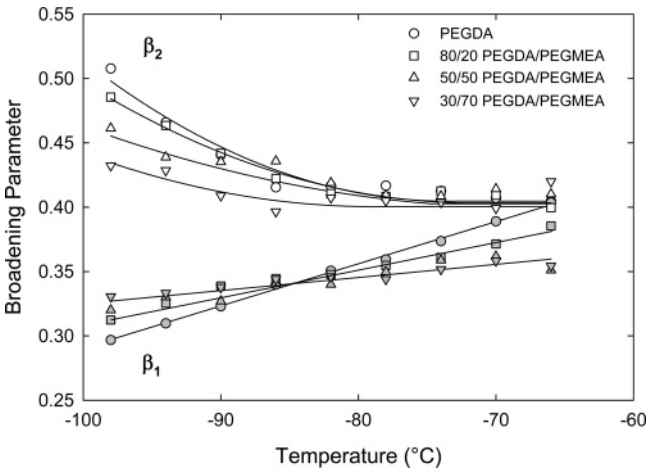

Figure 5. Havriliak−Negami [HN] broadening parameter vs temperature for PEGDA/PEGMEA copolymer networks. The broadening parameter corresponds to *a* in eq 1. β_1 [filled symbols] and β_2 [unfilled symbols] sub-glass transitions.

set equal to 1 in all cases; this corresponds to the symmetric Cole−Cole form of eq 1.[33]

The HN parameters for the PEGDA/PEGMEA series are plotted in Figure 4 (relaxation intensity; $\Delta\epsilon = \epsilon_R - \epsilon_U$) and Figure 5 (breadth), respectively. For both the β_1 and β_2 processes, the relaxation intensity increases with temperature (see Figure 4). Increasing the comonomer content leads to a decrease in $\Delta\epsilon$ for both dispersions, but the drop in intensity is much more pronounced for the β_2 relaxation, as discussed above. Examination of Figure 5 reveals a progressive narrowing of the β_1 process as indicated by the increase in broadening parameter, which reflects a tighter distribution of relaxation times with increasing thermal energy. The β_2 process, however, shows an overall broadening with increasing temperature that appears to be characteristic of this constrained relaxation. It is notable that as the PEGMEA content in the networks is reduced, this effect becomes weaker (see trend lines in Figure 5), a result that is consistent with the reduction in cross-link constraint at higher levels of comonomer incorporation.

The sub-glass relaxation results for the PEGDA/PEGA copolymer series are presented in Figure 6 (ϵ'' vs frequency at

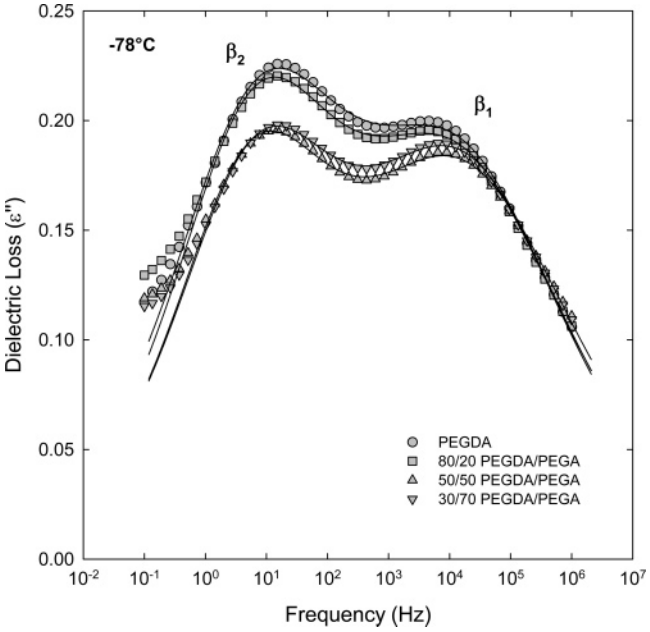

Figure 6. Dielectric loss (ϵ'') vs frequency for PEGDA/PEGA copolymer networks at −78 °C. Solid curves are dual HN fits.

−78 °C). Across this series of specimens, the influence of copolymer composition on relaxation intensity is not as strong as in the PEGDA/PEGMEA samples. For the PEGDA/PEGA copolymers, the introduction of PEGA branches leads to a reduction in FFV, possibly due to the formation of hydrogen bonds involving the −OH groups located at the ends of the PEGA segments. While the incorporation of the PEGA comonomer produces a decrease in overall cross-link density in the networks, the potential for interactions involving the branch ends results in the persistence of a significant degree of motional constraint. Accordingly, only a modest decrease in the intensity of the β_2 relaxation with comonomer content is observed for the PEGDA/PEGA series of copolymers.

The time−temperature characteristics of the β_1 and β_2 dispersions in PEGDA/PEGMEA and PEGDA/PEGA are presented as Arrhenius plots of $\log(f_{MAX})$ vs $1000/T$ (K) in Figure 7. For the symmetric sub-glass processes, f_{MAX} was determined directly from the individual HN curve fits, with $f_{MAX} = [2\pi\tau_{MAX}]^{-1}$. Both the β_1 and β_2 relaxations display a linear, Arrhenius time−temperature relationship that is consistent with a local relaxation process and which is typical of sub-glass relaxations in amorphous and semicrystalline polymers.[34,35] The positions of the β_1 and β_2 relaxations are nearly independent of copolymer composition, with a slightly greater spread in the data evident across the PEGDA/PEGMEA series. For the PEGDA/PEGA copolymers, the apparent activation energies (E_A) associated with the β_1 and β_2 processes are essentially the same as those previously reported for the 100% XLPEGDA network: $E_A(\beta_1) = 41$ kJ/mol and $E_A(\beta_2) = 65$ kJ/mol.[25] In the PEGDA/PEGMEA polymers, the activation energy for the β_1 process ranges from 41 kJ/mol (100% PEGDA) to 33 kJ/mol (30/70 PEGDA/PEGMEA), while the activation energy for the β_2 process is approximately constant at 65 kJ/mol. These values are quite similar to the sub-glass activation energies determined for crystalline PEO, where $E_A(\beta_1) = 32$ kJ/mol and $E_A(\beta_2) = 65$ kJ/mol.[25]

Analysis of Glass−Rubber Relaxation for PEGDA Copolymers. In the vicinity of the glass−rubber relaxation, there is significant overlap of the β and α processes as well as a sizable conduction contribution. A dual HN analysis was

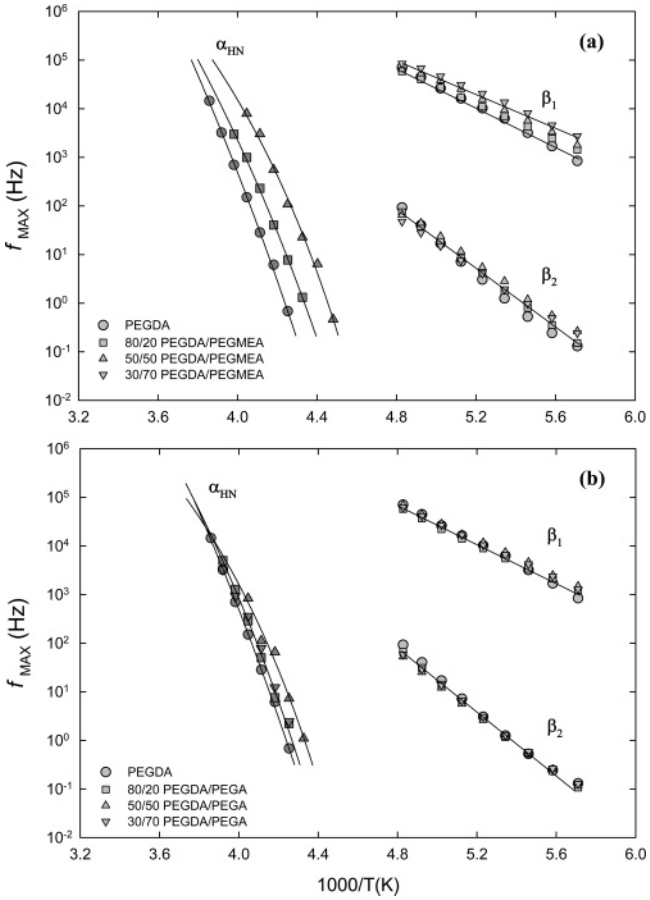

Figure 7. Arrhenius plot of f_{MAX} (Hz) vs 1000/T (K): **(a)** PEGDA/PEGMEA copolymer networks; **(b)** PEGDA/PEGA copolymer networks.

performed at discrete temperatures near T_g in order to establish the relaxation times (τ_{HN}) associated with the individual processes and to remove the influence of conduction. The governing equation is as follows:

$$\epsilon^* = \epsilon' - i\epsilon'' = \epsilon_{U_1} + \sum_{i=1}^{2} \frac{\epsilon_{R_i} - \epsilon_{U_i}}{[1 + (i\omega\tau_{HN_i})^{a_i}]^{b_i}} - i\left(\frac{\sigma}{\epsilon_0 \omega}\right) \quad (2)$$

where σ is the conductivity and ϵ_0 is the vacuum permittivity. For the merged β relaxation ($\beta_1 + \beta_2$), the skewing parameter (b) was always taken equal to 1, such that the relaxation time associated with the peak maximum, $\tau_{MAX} = \tau_{HN}$. For the glass−rubber (α) relaxation, high-frequency skewing was observed, and the skewing parameter assumed values, $b < 1$. In this case, the peak maximum relaxation time (τ_{MAX}) was determined from the HN best-fit parameters:[29]

$$\tau_{MAX} = \tau_{HN}\left[\frac{\sin\left(\frac{\pi ab}{2 + 2b}\right)}{\sin\left(\frac{\pi a}{2 + 2b}\right)}\right]^{1/a} \quad (3)$$

Dielectric loss data (−30 °C) and corresponding HN curve fits for the PEGDA/PEGMEA and PEGDA/PEGA copolymer series are plotted vs frequency in Figures 8 and 9, respectively. The data are shown with the conduction contribution removed according to eq 2.

Examination of the PEGDA/PEGMEA glass−rubber (α) relaxation in Figure 8 indicates a strong shift in the relaxation

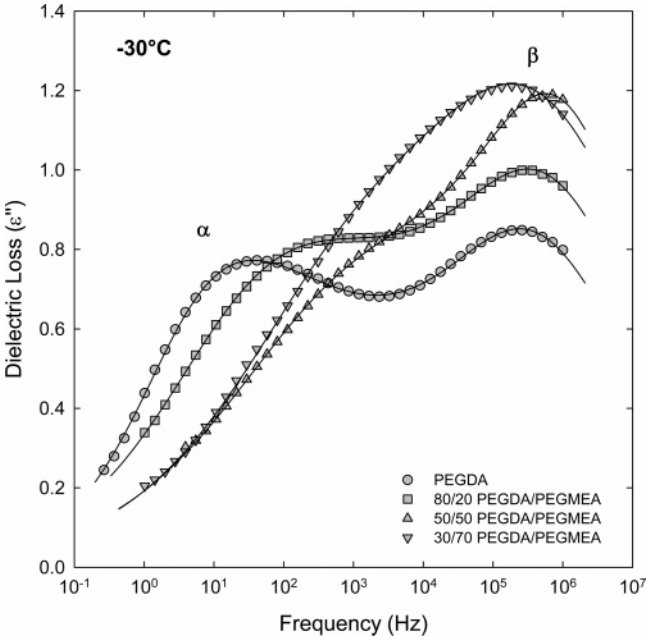

Figure 8. Dielectric loss (ϵ'') vs frequency for PEGDA/PEGMEA copolymer networks at −30 °C. Data are corrected for conduction contribution according to eq 2. Solid curves are dual HN fits.

maximum to higher frequencies (i.e., shorter relaxation times) that is consistent with the observed negative offset in T_g with increasing PEGMEA content (see Table 2). At lower cross-linker contents, there is extensive overlap between the relaxations owing to the shift in the α relaxation to higher frequencies. For the 30/70 PEGDA/PEGMEA specimen, a very broad relaxation curve is obtained at −30 °C. PEGDA/PEGMEA networks with high levels of PEGMEA and correspondingly low cross-link densities have a tendency to crystallize. Previous DMA scans on the 30/70 PEGDA/PEGMEA network, for example, display cold crystallization just above T_g;[11] a small degree of cold crystallization has also been detected in DSC scans on lightly cross-linked PEGDA/PEGMEA networks.[10] It is likely that a small amount of crystallinity is present in the 30/70 PEGDA/PEGMEA specimen examined via dielectric spectroscopy, evolving either during the initial cooling of the specimen or possibly as cold crystallization in the course of measurements just above T_g. The presence of crystallinity would be expected to subject the responding chain segments to additional constraint, shifting the glass transition to higher temperatures (i.e., lower frequencies) and broadening the relaxation.[35] Both effects are evident in the 30/70 PEGDA/PEGMEA dispersion recorded at −30 °C.

The dielectric loss curves for the PEGDA/PEGA networks (−30 °C; see Figure 9) show a somewhat clearer separation between the α and β relaxations across the series of copolymer specimens: in this case, the position of the α relaxation is less sensitive to composition, resulting in a lower degree of $\alpha-\beta$ overlap at higher PEGA comonomer content. The intensities of both the α and β dispersions increase with increasing PEGA, although this trend reverses for the 30/70 copolymer (i.e., intensities for the 30/70 PEGDA/PEGA sample are lower than those for the 50/50 network). This behavior may reflect competing structural factors that influence the net dielectric response. Although the overall chemical constitution of the PEGDA networks remains constant across each series, decreasing cross-link density correlates with an increase in the measured dielectric intensity, most likely due to increased mobility of the (−COO−) ester linkages located at the cross-link junctions.

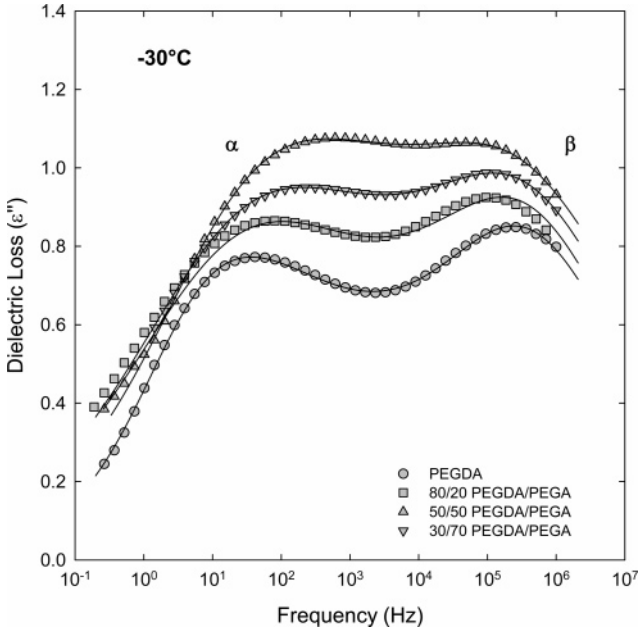

Figure 9. Dielectric loss (ϵ'') vs frequency for PEGDA/PEGA copolymer networks at −30 °C. Data are corrected for conduction contribution according to eq 2. Solid curves are dual HN fits.

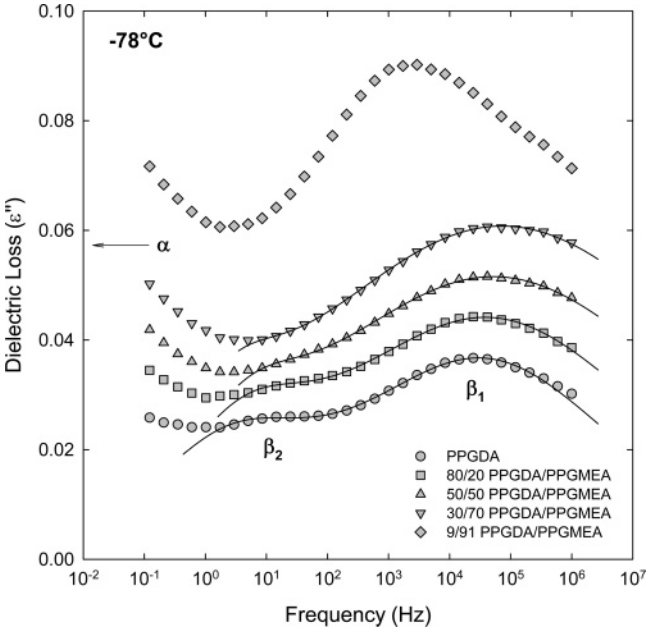

Figure 10. Dielectric loss (ϵ'') vs frequency for PPGDA/PPGMEA copolymer networks at −78 °C. Solid curves are dual HN fits.

However, in the case of the 30/70 PEGDA/PEGA sample, the large number of −OH-terminated PEGA branches, and the potential formation of hydrogen bonds involving these terminal groups, may be responsible for a decrease in dipolar mobility as compared to the 50/50 PEGDA/PEGA copolymer. The result, as seen in Figure 9, is a net reduction in dielectric intensity, driven primarily by a decrease in the strength of the α relaxation response.

The peak maxima associated with the α and β relaxations were determined across a range of temperatures in the vicinity of the glass transition (−14 to −50 °C, depending on composition). The results for the α relaxation are plotted as $f_{MAX} = [2\pi\tau_{MAX}]^{-1}$ vs reciprocal temperature in Figure 7, where τ_{MAX} was determined from the individual HN curve fits according to eq 3. For the PEGDA/PEGMEA and PEGDA/PEGA series, the α relaxation displays time−temperature characteristics that are consistent with a cooperative reorientation response and which can be described by the Vogel−Fulcher−Tammann (VFT) relation (see solid curves in Figure 7).[36] In both cases, the relative positions of the relaxation curves, which shift to higher values of reciprocal temperature with decreasing cross-linker content, are consistent with the glass transition results measured by DMA and DSC.[10,11] The offset in the curves is greater for the PEGDA/PEGMEA polymers, in direct correspondence to the data presented in Table 2.

Dielectric Results for PPGDA/PPGMEA Copolymers. The PPGDA/PPGMEA rubbery copolymer networks, based on the monomers shown in Table 1, differ from the PEGDA series in a number of respects: (i) the 100% cross-linked network, XLPPGDA, encompasses a much higher degree of fractional free volume as compared to XLPEGDA (see Table 2); (ii) the PPGMEA comonomer molecular weight is relatively low, such that much shorter pendant branches ($n = 2$) are inserted into the network; and (iii) the introduction of PPGMEA comonomer to the reaction mixture results in a change in the chemical composition of the network, with increasing PPGMEA content leading to an increase in the relative population of (−COO−) linkages.

Figure 10 shows dielectric loss plotted vs frequency for the PPGDA/PPGMEA series in the sub-glass transition range (−78 °C). For XLPPGDA and the PPGDA-based copolymers, the intensities of the sub-glass transitions are much weaker than those encountered in XLPEGDA, and this is consistent with the character of the sub-glass process observed in un-cross-linked PPO polymer[37−39] (see the discussion in ref 25). Two distinct sub-glass transitions are evident in the PPGDA copolymer networks, with the position of the β_2 process quite close to the "fast" relaxations observed in XLPEGDA and PEO. The β_2 relaxation in XLPPGDA and its copolymers likely has the same underlying origin as the β_2 process observed in the PEGDA copolymers and would presumably display a comparable sensitivity to copolymer composition and the corresponding degree of constraint imposed by the network junctions. Examination of Figure 10 reveals that the relative intensity of the β_2 process is diminished with decreasing cross-linker content, in a manner similar to that observed for the PEGDA/PEGMEA and PEGDA/PEGA series: as the overall network structure is loosened, fewer segments adopt conformations that contribute to the "fast" relaxation response. Unfortunately, the strong degree of overlap between the β_1 and β_2 dispersions makes it difficult to reliably determine the HN broadening parameters associated with the individual relaxations at lower PPGDA content. However, for the 100% XLPPGDA network, the HN broadening parameter for the β_2 relaxation displays the same trend with temperature that was observed for PEO and the PEGDA copolymers and which is consistent with the β_2 process originating at the constrained cross-link junctions.[25]

Owing to the relatively weak intensity of the sub-glass processes in the PPGDA/PPGMEA copolymers, the dielectric spectra for these materials can be fit in the range of the glass transition using a single HN function. Representative dielectric loss data (−30 °C) and corresponding HN curve fits for these polymers are plotted vs frequency in Figure 11; HN best fits in the glass transition region were used to establish the value of τ_{MAX} for each copolymer as a function of temperature. Increasing amounts of PPGMEA in the copolymers lead to an enhancement in the intrinsic polarizability of the networks, as manifested by a progressive increase in the unrelaxed value of the dielectric constant, ϵ_U, as determined from the HN fits. The intensity of the glass−rubber (α) relaxation increases systemati-

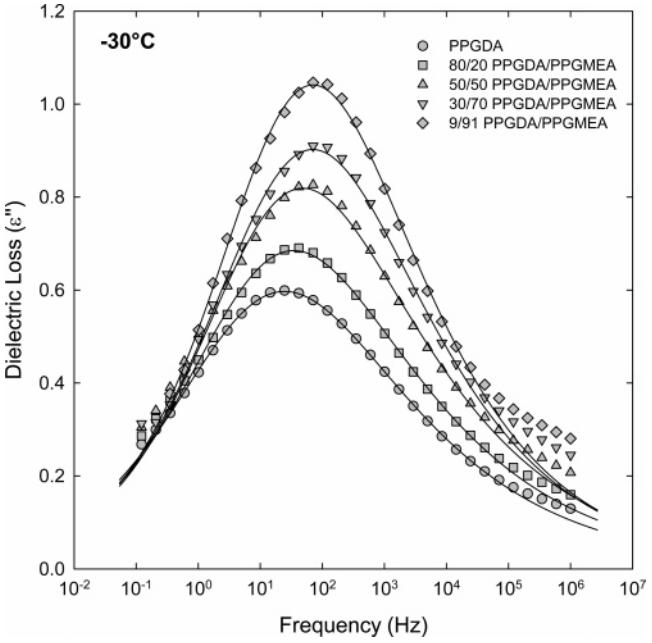

Figure 11. Dielectric loss (ϵ'') vs frequency for PPGDA/PPGMEA copolymer networks at −30 °C. Solid curves are dual HN fits.

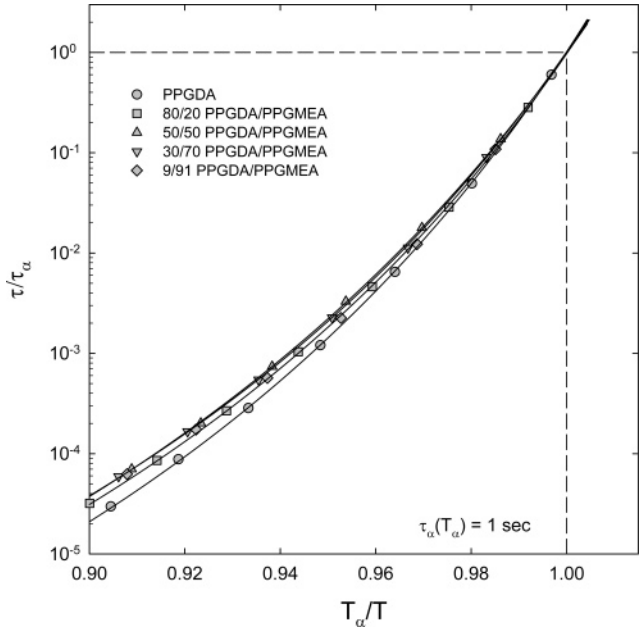

Figure 12. Cooperativity plots of τ/τ_α vs T_α/T for PPGDA/PPGMEA copolymer networks. Solid curves are VFT fits.

cally with increasing PPGMEA content owing to both an increase in the number of (−COO−) ester moieties present in the network as well as a likely increase in dipolar mobility with increasing fractional free volume. However, there is little variation in the dielectric peak position as a function of copolymer composition, which is consistent with the relatively constant values of glass transition temperature for this system measured via calorimetric and dynamic mechanical methods (see Table 2).[15]

The time−temperature characteristics of the PPGDA/PPGMEA networks can be compared by the construction of cooperativity or fragility plots, which are normalized Arrhenius plots wherein relaxation time (τ_{MAX}/τ_α) is plotted vs reciprocal temperature (T_α/T).[16,40] In this context, T_α is the glass transition temperature, and τ_α is the relaxation time associated with T_α. For the dielectric measurements reported here, we adopt a convention whereby T_α is the transition temperature associated with a value of the relaxation time, $\tau_\alpha = 1$ s. The cooperativity plots for XLPPGDA and its copolymers are presented in Figure 12, with the solid curves corresponding to VFT fits to the data. The apparent activation energy for the individual networks can be determined by evaluating the slope of each data curve at $T = T_\alpha$. For the 100% XLPPGDA network, an apparent activation $E_A = 310$ kJ/mol is obtained from the dielectric data, which is very close to the value determined from DMA measurements (i.e., 300 kJ/mol) where T_α was assigned to the dynamic mechanical peak temperature at 1 Hz.[15] Across the PPGDA/PPGMEA copolymer series, a progressive decrease in apparent activation energy is observed with decreasing cross-link density: this trend is consistent with our previous DMA results for the PEGDA[11] and PPGDA[15] copolymers and has been reported in the literature for other cross-linked homopolymer systems.[16,17,24] For the PPGDA/PPGMEA dielectric data reported here, an apparent activation energy $E_A = 280$ kJ/mol is obtained for the 80/20 copolymer composition, and an E_A value of 250 kJ/mol is obtained for the 50/50, 30/70, and 9/91 PPGDA/PPGMEA copolymers. The introduction of PPGMEA into the network leads to a reduction in the cooperativity inherent to the glass transition with decreasing effective cross-link density. The net impact of copolymerization with the acrylate comonomer is an overall increase in fractional free volume and a decrease in the degree of constraint imposed by the cross-link junctions such that less segmental cooperation is required across the glass−rubber relaxation.

Conclusions

The relaxation characteristics of amorphous copolymer networks based on PEGDA and PPGDA cross-linkers have been investigated by dielectric relaxation spectroscopy. The glass−rubber and sub-glass relaxation processes in these networks are sensitive to the details of the network architecture, including branch length and the nature and character of the branch end groups. For the PEGDA-based networks, the inclusion of acrylate comonomer in the prepolymerization reaction mixture and corresponding insertion of flexible branch groups in the resulting cross-linked networks led to a decrease in the measured glass−rubber relaxation temperature and an overall increase in dielectric relaxation intensity with reduced cross-link density. In both the PEGDA- and PPGDA-based networks, an intermediate sub-glass relaxation (i.e., the β_2 process) was observed that was analogous to a "fast" sub-T_g relaxation detected in crystalline PEO and which has been attributed to a subset of noncooperative segmental reorientations originating in the vicinity of the cross-link junctions. The measured intensity of the β_2 process decreased with increasing comonomer content owing to a loosening of the constraint imposed by the network junctions at lower effective cross-link density. A characteristic broadening of the β_2 relaxation was observed with increasing temperature that reflected the contrasting mobility of the flexible and constrained regions of the network; this distinctive broadening behavior was less pronounced in those copolymers containing lower degrees of cross-linking. For the short-branched PPGDA networks, dielectric relaxation intensity increased strongly with comonomer content across the glass transition region owing to an increase in the number of (−COO−) ester dipoles present along the network backbone. Normalized cooperativity plots indicated a progressive decrease in the dynamic fragility of the networks (i.e., lower apparent activation energy at T_g) with decreased cross-link density, a result that was consistent with previous dynamic mechanical studies.

Acknowledgment. We are pleased to acknowledge support from the Kentucky Science and Engineering Foundation as per Grant Agreement KSEF-148-502-05-130 with the Kentucky Science and Technology Corporation. This study was also supported through a Major Research Equipment Grant awarded by the Office of the Vice President for Research at the University of Kentucky. Activities at the University of Texas were supported in part by the Chemical Sciences, Geosciences and Biosciences Division, Office of Basic Energy Sciences, Office of Science, U.S. Department of Energy (Grant DE-FG02-02ER15362). However, any opinions, findings, conclusions, or recommendations expressed herein are those of the authors and do not necessarily reflect the views of the DOE. Partial support from the National Science Foundation under Grant CTS-0515425 is also acknowledged.

References and Notes

(1) Kremer, F.; Arndt, M. In *Dielectric Spectroscopy of Polymeric Materials: Fundamentals and Applications*; Runt, J. P., Fitzgerald, J. J., Eds.; American Chemical Society: Washington, DC, 1997; pp 67−79.
(2) Kremer, F.; Schonhals, A. In *Broadband Dielectric Spectroscopy*; Kremer, F., Schonhals, A., Eds.; Springer-Verlag: Berlin, 2003; pp 35−57.
(3) Kranbuehl, D. E. In *Dielectric Spectroscopy of Polymeric Materials: Fundamentals and Applications*; Runt, J. P., Fitzgerald, J. J., Eds.; American Chemical Society: Washington, DC, 1997; pp 303−328.
(4) Mijovic, J. In *Broadband Dielectric Spectroscopy*; Kremer, F., Schonhals, A., Eds.; Springer-Verlag: Berlin, 2003; pp 349−384.
(5) Lin, H.; Freeman, B. D. *J. Membr. Sci.* **2004**, *239*, 105−117.
(6) Lin, H.; Freeman, B. D. *J. Mol. Struct.* **2005**, *739*, 57−74.
(7) Lin, H.; Freeman, B. D. *Macromolecules* **2005**, *38*, 8394−8407.
(8) Lin, H.; Freeman, B. D. *Macromolecules* **2006**, *39*, 3568−3580.
(9) Lin, H.; Kai, T.; Freeman, B. D.; Kalakkunnath, S.; Kalika, D. S. *Macromolecules* **2005**, *38*, 8381−8393.
(10) Lin, H.; Van Wagner, E.; Swinnea, J. S.; Freeman, B. D.; Pas, S. J.; Hill, A. J.; Kalakkunnath, S.; Kalika, D. S. *J. Membr. Sci.* **2006**, *276*, 145−161.
(11) Kalakkunnath, S.; Kalika, D. S.; Lin, H.; Freeman, B. D. *Macromolecules* **2005**, *38*, 9679−9687.
(12) Kalakkunnath, S.; Kalika, D. S.; Lin, H.; Freeman, B. D. *J. Polym. Sci., Part B: Polym. Phys.* **2006**, *44*, 2058−2070.
(13) Lin, H.; Van Wagner, E.; Raharjo, R.; Freeman, B. D.; Roman, I. *Adv. Mater.* **2006**, *18*, 39−44.
(14) Lin, H.; Van Wagner, E.; Freeman, B. D.; Toy, L. G.; Gupta, R. P. *Science* **2006**, *311*, 639−642.
(15) Raharjo, R. D.; Lin, H.; Sanders, D. F.; Freeman, B. D.; Kalakkunnath, S.; Kalika, D. S. *J. Membr. Sci.* **2006**, *283*, 253−265.
(16) Roland, C. M. *Macromolecules* **1994**, *27*, 4242−4247.
(17) Schroeder, M. J.; Roland, C. M. *Macromolecules* **2002**, *35*, 2676−2681.
(18) Fitz, B. D.; Mijovic, J. *Macromolecules* **1999**, *32*, 3518−3527.
(19) Kannurpatti, A. R.; Anderson, K. J.; Anseth, J. W.; Bowman, C. N. *J. Polym. Sci., Part B: Polym. Phys.* **1997**, *35*, 2297−2307.
(20) Kannurpatti, A. R.; Anseth, J. W.; Bowman, C. N. *Polymer* **1998**, *39*, 2507−2513.
(21) Kannurpatti, A. R.; Bowman, C. N. *Macromolecules* **1998**, *31*, 3311−3316.
(22) Glatz-Reichenbach, J. K. W.; Sorriero, L. J.; Fitzgerald, J. J. *Macromolecules* **1994**, *27*, 1338−1343.
(23) Litvinov, V. M.; Dias, A. A. *Macromolecules* **2001**, *34*, 4051−4060.
(24) Alves, N. M.; Gomez Ribelles, J. L.; Gomez Tejedor, J. A.; Mano, J. F. *Macromolecules* **2004**, *37*, 3735−3744.
(25) Kalakkunnath, S.; Kalika, D. S.; Lin, H.; Raharjo, R. D.; Freeman, B. D. *Polymer* **2007**, *48*, 579−589.
(26) Jin, X.; Zhang, S.; Runt, J. *Polymer* **2002**, *43*, 6247−6254.
(27) Vaia, R. A.; Sauer, B. B.; Tse, O. K.; Giannelis, E. P. *J. Polym. Sci., Part B: Polym. Phys.* **1997**, *35*, 59−67.
(28) Elmahdy, M. M.; Chrissopoulou, K.; Afratis, A.; Floudas, G.; Anastasiadis, S. *Macromolecules* **2006**, *39*, 5170−5173.
(29) Schonhals, A.; Kremer, F. In *Broadband Dielectric Spectroscopy*; Kremer, F., Schonhals, A., Eds.; Springer-Verlag: Berlin, 2003; pp 59−98.
(30) Schonhals, A. In *Dielectric Spectroscopy of Polymeric Materials: Fundamentals and Applications*; Runt, J. P., Fitzgerald, J. J., Eds.; American Chemical Society: Washington, DC, 1997; pp 81−106.
(31) Havriliak, S.; Negami, S. *J. Polym. Sci., Polym. Symp.* **1966**, *14*, 99−103.
(32) Havriliak, S.; Havriliak, S. J. *Dielectric and Mechanical Relaxation in Materials*; Hanser: Cincinnati, 1997.
(33) Cole, K. S.; Cole, R. H. *J. Chem. Phys.* **1941**, *9*, 341−351.
(34) McCrum, N. G.; Read, B. E.; Williams, G. *Anelastic and Dielectric Effects in Polymeric Solids*; John Wiley and Sons: London, 1967.
(35) Kalika, D. S. In *Handbook of Low and High Dielectric Constant Materials and Their Applications*; Nalwa, H. S., Ed.; Academic Press: New York, 1999; Vol. 1, pp 275−327.
(36) Kremer, F.; Schonhals, A. In *Broadband Dielectric Spectroscopy*; Kremer, F., Schonhals, A., Eds.; Springer-Verlag: Berlin, 2003; pp 99−129.
(37) Johari, G. P. *Polymer* **1986**, *27*, 866−870.
(38) Leon, C.; Ngai, K. L.; Roland, C. M. *J. Chem. Phys.* **1999**, *110*, 11585−11591.
(39) Mattsson, J.; Bergman, R.; Jacobsson, P.; Borjesson, L. *Phys. Rev. Lett.* **2003**, *90*, 0757021−0757024.
(40) Angell, C. A. *J. Non-Cryst. Solids* **1991**, *131−133*, 13−31.

MA070016A